B31G-0546

The impact of the 2015-2016 El Niño-Southern Oscillation (*ENSO*) event on greenhouse gas exchange and surface energy budget in an Indonesian oil palm plantation

Christian Stiegler (1), Ana Meijide (1,2), Tania June (3), Alexander Knohl (1)

(1) Bioclimatology, University of Göttingen, Göttingen, Germany; (2) Department of Ecology, University of Granada, Granada, Spain; (3) Department of Geophysics and Meteorology, Bogor Agricultural University, Bogor, Indonesia

University of Göttingen · Bogor Agricultural University · University of Jambi · Tadulako University

DFG Deutsche Forschungsgemeinschaft

1 Background

The 2015-2016 El Niño-Southern Oscillation (*ENSO*) event was one of the strongest observed in the last 20 years. Oil palm plantations cover a large fraction of lowlands in Southeast Asia but despite their growing areal extent, measurements of greenhouse gas exchange and surface energy balance are still scare. Further, the effects of *ENSO* on carbon sequestration and partitioning of energy balance components are widely unknown.

2 Study aim

Investigate surface energy and greenhouse gas exchange in an Indonesian oil palm plantation before and during the 2015-2016 *ENSO* event.

3 Materials and methods

Study site:

The study site and climate measurement tower is located in a commercial oil palm plantation (*PTPN6*) in the tropical lowlands of the Jambi province on Sumatra, Indonesia (**Fig. 1**). The terrain is generally flat with small elevation variations (± 15 meters).
The total oil palm plantation covers approx. 2000 ha. Oil palms were planted between the years 1999 and 2004. Average oil palm height is approx. 12 meters.

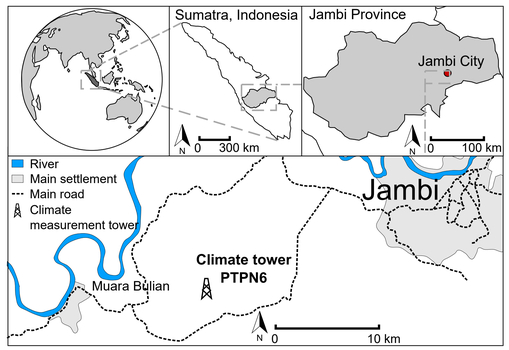

Fig. 1: Map and location of the study site and climate measurement tower in the Hararapan Landscape, approx. 15 km south-west of the city of Jambi (Sumatra, Indonesia).

Measurement setup and measured parameters:

Fig. 2: Climate measurement tower (**A**), top-of-tower view (**B**), below-canopy structure (**C**).

Parameter	Sensor	Instrument height or depth
Wind speed & direction	uSonic-3 Scientific (Metek), Thies Clima	22 m
Water vapor and CO_2 fluxes	LI7500A (LI-COR Inc.)	22 m
Ground heat flux	HFP01 (Hukseflux)	-5 cm
Radiation	CNR4 (Kipp & Zonen)	22 m
PAR	PQS1 (Kipp & Zonen)	22 m
Air temperature & humidity	Thies Clima	22 m
Precipitation	Thies Clima	11.5 m

Table 1: Meteorological measurements, instrument type and sensor height or depth.

Data collection and processing:

- Continuous measurements of greenhouse gas exchange, surface energy balance components and meteorological parameters were performed since June 2014.
- Concentration of water vapor and CO_2, sonic temperature and wind components *u*, *v* and *w* were sampled at a rate of 10 Hz. Fluxes were calculated for 30-minute intervals using the EddyPro 6.2.0 software package. Standard flux processing and data quality checks have been performed. Missing values were filled using online gap-filling (MPI).
- Climatic variables and ground heat fluxes were measured every 15-s and averaged to 10- and 30-minute intervals.

4 Results and discussion

Meteorological parameters and Multivariate *ENSO*-Index (*MEI*):

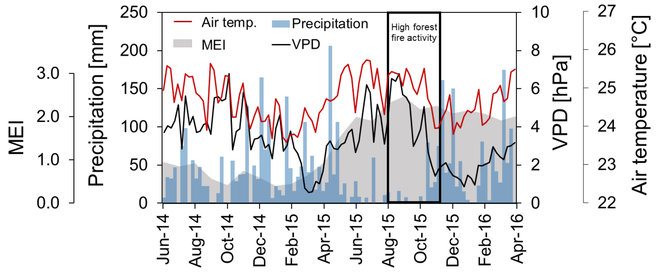

Fig. 3a: 7-day average of air temperature and vapor pressure deficit (*VPD*), 7-day accumulated precipitation, and monthly values of Multivariate *ENSO*-Index (*MEI*) during the period 1 June 2014 to 1 April 2016.

Fig. 3b: Haze of smoke in the city of Jambi during the peak of forest fires. (Photo: Dr. Katja Rembold)

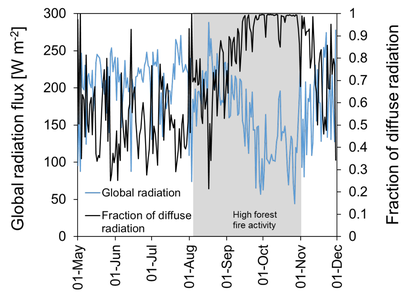

Fig. 3c: Daily average of global radiation and fraction of diffuse radiation during the period 1 May to 1 December 2015. The period 3 August to 31 October 2015 is characterized by high forest fire activity (gray area).

Air temperature and vapor pressure deficit (*VPD*) generally decrease until March 2015 when *MEI* is low (**Fig. 3a**). The following strong increase in *MEI* until August 2015 coincides with increasing air temperature and *VPD*. Low precipitation from May to October 2015 promotes favorable conditions for forest fires, resulting in strong haze of smoke (**Fig. 3b**).

As *MEI* increases, the diffuse fraction of the shortwave radiation flux is approx. 0.5, with strong day-to-day variations (**Fig. 3c**).
With increasing forest fire activity and haze of smoke, these day-to-day variations decrease and diffuse radiation becomes almost the sole shortwave radiation flux while absolute values of global radiation strongly decrease.

Surface energy balance components:

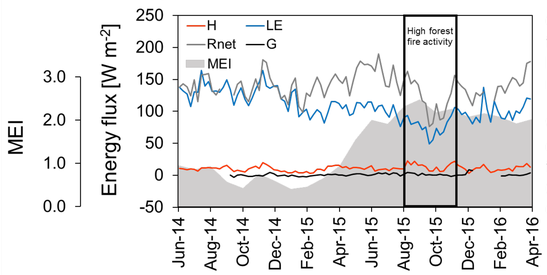

Fig. 4a: 7-day average of sensible heat flux (*H*), latent heat flux (*LE*), net radiation (*Rnet*), ground heat flux (*G*), and monthly values of Multivariate *ENSO*-Index (*MEI*) during the period 1 June 2014 to 1 April 2016.

Over the entire observation period, latent heat flux (*LE*) is the dominant heat flux while sensible heat flux (*H*) and ground heat flux (*G*) play only a minor role in the surface energy budget (**Fig. 4a**).

With increasing *MEI*, Bowen ratio (*H*/*LE*) remains constant, however, in the beginning of the high forest fire activity, *H*/*LE* generally increases (**Fig. 4b, 4c**) as high net radiation (*Rnet*) and dry conditions promote *H* at the cost of *LE*.

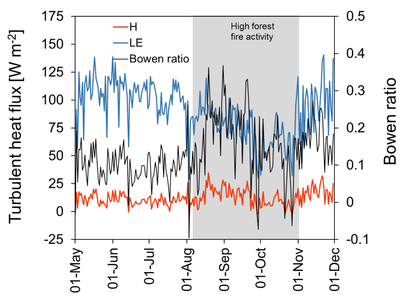

Fig. 4b: Daily average of sensible heat flux (*H*), latent heat flux (*LE*) and Bowen ratio (*H*/*LE*) during the period 1 May to 1 December 2015. The period 3 August to 31 October 2015 is characterized by high forest fire activity (gray area).

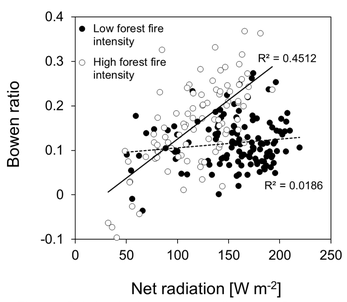

Fig. 4c: Relationship between net radiation and Bowen ratio (*H*/*LE*) during low forest fire intensity and during high forest fire intensity.

Net ecosystem exchange (*NEE*) and photosynthetically active radiation (*PAR*):

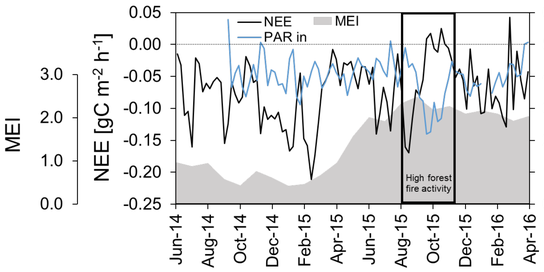

Fig. 5a: 7-day average of net ecosystem exchange (*NEE*) and incoming photosynthetically active radiation (*PAR in*), and monthly values of Multivariate *ENSO*-Index (*MEI*) during the period 1 June 2014 to 1 April 2016.

During the entire observation period *NEE* shows strong daily and weekly variations, with no clear trend as *MEI* increases (**Fig. 5a**).

During the period of high forest fire activity, carbon uptake increases at first as clear-sky conditions allow high incoming *PAR* (**Fig. 5b, 5c**). Strong haze of smoke, and related low incoming *PAR*, turn the oil palm plantation into a source of carbon.

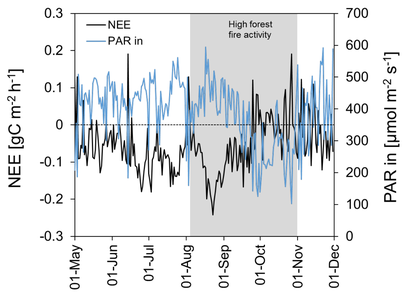

Fig. 5b: Daily average of net ecosystem exchange (*NEE*) and incoming photosynthetically active radiation (*PAR in*) during the period 1 May to 1 December 2015. The period 3 August to 31 October 2015 is characterized by high forest fire activity (gray area).

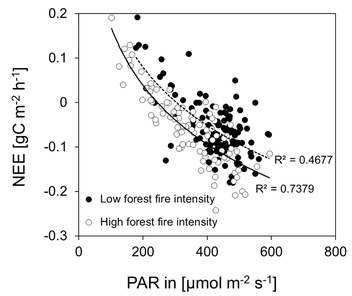

Fig. 5c: Relationship between net ecosystem exchange (*NEE*) and incoming photosynthetically active radiation (*PAR in*) during low forest fire intensity and during high forest fire intensity.

5 Summary and conclusion

	Pre-*ENSO* (*MEI* <1)	Pre-forest fire	High forest fire activity		Post-forest fire
			3 Aug. - 15 Sept. 2015	16 Sept. - 31 Oct. 2015	
Multivariate *ENSO*-Index (*MEI*)	0.71 ± 0.21	1.88 ± 0.21	2.41 ± 0.12	2.23 ± 0.0	2.14 ± 0.11
Fraction of diffuse radiation	0.72 ± 0.19	0.52 ± 0.16	0.82 ± 0.18	0.98 ± 0.03	0.70 ± 0.18
Net radiation (*Rnet*), W m^{-2}	136.7 ± 39.0	162.0 ± 33.7	124.2 ± 35.5	89.9 ± 28.4	136.8 ± 39.3
Sensible heat flux (*H*), W m^{-2}	9.7 ± 6.2	10.5 ± 5.0	13.6 ± 8.1	6.8 ± 5.3	11.4 ± 7.6
Latent heat flux (*LE*), W m^{-2}	122.2 ± 29.2	104.4 ± 17.3	75.3 ± 18.4	65.7 ± 18.9	98.2 ± 24.4
Bowen ratio (*H*/*LE*)	0.08 ± 0.06	0.10 ± 0.04	0.17 ± 0.09	0.09 ± 0.07	0.11 ± 0.09
Net ecosystem exchange (*NEE*), gC m^{-2} h^{-1}	-0.09 ± 0.08	-0.07 ± 0.07	-0.06 ± 0.08	0.01 ± 0.08	-0.06 ± 0.09
Incoming *PAR*, µmol m^{-2} s^{-1}	399.3 ± 104.4	428.5 ± 75.4	362.5 ± 107.7	268.3 ± 81.5	399.3 ± 104.7

Table 2: Details of meteorological parameters, radiation components, heat fluxes and net ecosystem exchange during different periods of the overall study period. Means and standard deviation were derived from daily averages.

Different response of surface energy balance and net ecosystem exchange to changes in atmospheric conditions and radiative components driven by *ENSO*:

- **Increasing *ENSO*-intensity and related clear-sky condtitions:**
  - High ecosystem productivity, high net radiation, constant Bowen ratio
- **Low precipitation, increasing intensity of forest fires:**
  - Clear shift in the behavior of the oil palm plantation, e.g. source of carbon to the atmosphere, increasing Bowen ratio, diffuse radiation almost sole shortwave radiation component
- **Post-forest fire period:**
  - Similar behavior of net ecosystem exchange and surface energy balance compared with pre-forest fire period

References

Wolter, K., Multivariate ENSO Index (MEI), U.S. Department of Commerce, National Oceanic and Atmospheric Administration, Earth System Research Laboratory, Physical Sciences Division, www.esrl.noaa.gov/psd/enso/mei/

NASA Fire Information for Resource Management (FIRMS) Active Fire Data, earthdata.nasa.gov/earth-observation-data/near-real-time/firms

REddyProc: Eddy covariance data processing tool, Department of Biogeochemical Integration at MPI Jena, http://www.bgc-jena.mpg.de/REddyProc/brew/REddyProc.rhtml

Contact

Christian Stiegler, PhD
Department of Bioclimatology,
University of Göttingen, Germany
christian.stiegler@biologie.uni-goettingen.de
www.uni-goettingen.de/bioclimatology

Acknowledgements

This study is funded by *DFG Deutsche Forschungsgemeinschaft* and *Collaborative Research Center 990, University of Göttingen*